Prepared for submission to JCAP

Willman 1: An X-ray shot in the dark with Chandra

D. Nieto[a] **and N. Mirabal**[a,b]

[a]Dpto. de Física Atómica, Molecular y Nuclear, Universidad Complutense de Madrid, Spain
[b]Ramón y Cajal Fellow

E-mail: nieto@gae.ucm.es, mirabal@gae.ucm.es

Abstract. The sterile neutrino is a weakly-interacting particle that emerges in the framework of certain extensions of standard particle physics and that fits naturally with the properties of a warm dark matter particle candidate. We present an analysis of a deep archival *Chandra* observation of Willman 1, one of the darkest ultra-faint dwarf galaxies up to date, to exclude the presence of sterile neutrinos in the 1.6–16 keV mass range within 55 pc of its center down to the limiting flux of the observation. Spectral analysis of the *Chandra* data fails to find any non-instrumental spectral feature possibly connected with the radiative decay of a dark matter particle. Accordingly, we establish upper bounds on the sterile neutrino parameter space and discuss it in the context of previous measurements. Regarding the point source population, we identify a total of 26 sources within the central $5^{'}$ to a limiting $0.5-2.0$ keV X-ray flux of 6×10^{-16} erg cm^{-2} s^{-1}. While some of these sources could be formal members of Willman 1, we find no outstanding evidence for either an unusual population of bright X-ray sources or a densely populated cluster core. In fact, the entire X-ray population could be explained by background active galactic nuclei and/or foreground stars unrelated to Willman 1. Finally, possible associations of the X-ray point like population with optical sources from the *SDSS DR7* catalogue are presented.

Keywords: X-rays: general – galaxies: dwarfs galaxies – galaxies: individual (Willman 1) – cosmology: dark matter

ArXiv ePrint: 1003.3745

Contents

1 Introduction

There is strong evidence for the existence of dark matter (DM) in the Universe. In the concordance cosmological model (CCM), 83% of the mass density in the Universe cannot be explained with ordinary baryonic matter and requires an additional non-baryonic component [1]. Without a doubt, understanding DM is one of the most important topics of physics today [2, 3]. In the search for DM, three different approaches coexist: direct production in collider experiments [4], direct detection through scattering off ordinary matter [5], and indirect detection based on the search for secondary particles produced by the annihilation or decay of DM particles [6].

Within the last category, indirect searches for supersymmetric particles at center-of-mass energies between 10 GeV and a few TeV from pair annihilations or particle decays are being performed through gamma-ray observations of astrophysical objects with high dark matter density [7, 8]. While no significant dark matter signal has been verified using gamma-ray photons as messenger particles [9] some intriguing claims have emerged from measurements of the cosmic-rays positron fraction [10, 11] and electron spectrum in the same energy range [12, 13].

There are several theories offering DM particle candidates which can annihilate into standard model particles and eventually produce photons and leptons at energies above 10 GeV. A neutralino in the supersymmetric extensions of the standard model [14] or the Kaluza-Klein particle emerging from universal extra dimension theories [15] are two well known examples of cold dark matter (CDM) particle candidates. However, since the nature of the DM particle remains uncertain, one must broaden the range of hypothesised candidates/signatures taking in consideration options outside the gamma-ray regime [16]. If we move to the X-ray band, a possible candidate emerges in the form of the sterile neutrino. Sterile neutrinos are weakly-interacting fermions which arise as the right-handed counterparts of the standard neutrinos in some extensions of the standard model of particles. The lightest of these might lie in the keV range and would be compatible with a warm dark matter (WDM) candidate [17]. The sterile neutrino, besides qualifying as a good WDM particle candidate and resolving the neutrino mass problem, overcomes the puzzle of baryon asymmetry in some of these extensions of the standard model [18] and may mitigate some of the shortcomings of cold dark matter cosmologies including the apparent dearth of dwarf galaxies around the Milky Way [but see 19].

Sterile neutrinos decay in a two-body final state composed by a standard neutrino and a photon. Therefore, compact regions with significant accumulations of sterile neutrinos could "shine" in X-rays, producing a detectable X-ray flux line in the 0.1–100 keV energy range [20–22]. Ultimately, if the sterile neutrino is ever found in collider experiments, a clear identification of this particle in dense astrophysical regions would have to follow [23]. As we have discussed above, an unidentified X-ray line could be an invaluable DM smoking gun.

Since we are dealing with a decay, the subsequent line flux is directly proportional to the density of the DM region. Hence, astrophysical objects with the highest DM density are the favoured targets. Another condition that one should take into account when defining the best targets is whether the expected X-ray signal would be accompanied by any unrelated source of background that could eventually curtain a sterile neutrino signal. Accordingly, the most prominent targets to date are the recently discovered ultrafaint dwarf galaxies around the Milky Way [24, 25]. These objects, whose kinematic properties are still under study [26], could be the closest and densest dark matter structures in the Local Group, making them excellent targets to conduct DM searches [26, 27]. Additionally, their low baryonic content could minimise any external X-ray background. Nonetheless these predictions must be verified through careful study of the diffuse and point-like X-ray emission coming from these objects.

Indirect searches for sterile neutrinos in dwarf galaxies have been conducted in Fornax [28], Ursa Minor [29], Willman 1 [30], and Segue 1 [31]. Here, we perform such a search using a deep archival *Chandra* observation of the enigmatic Willman 1 [24], an ultra-faint object discovered in the *Sloan Digital Sky Survey* (*SDSS*) and originally classified as a dwarf galaxy [24, 32]. The arganization of the paper is as follows. §2 describes the X-ray observations. In §3 we discuss the diffuse component of Willman 1 and derive the parameter space for sterile neutrinos allowed by the data. The X-ray point source population and spectral analyses are explained in §4. Summary and conclusions are presented in §5.

2 Observations

Willman 1 was observed by the *Chandra X-ray Observatory* for 102.75 ks on 2009 January 27–28 (*Chandra* ObsID 10534) as described in **(author?)** [30]. Observations were conducted with the Advanced CCD Imaging Spectrometer (ACIS) in very faint (*VFAINT*) mode. Chips 0,1,2,3,6,7 were used with Willman 1 positioned near the ACIS-I aimpoint on the ACIS-I3 chip. Data reduction was performed using standard procedures[1] within the *Chandra* Interactive Analysis of Observations (CIAO) software. The level 1 event file was reprocessed to include grades 0,2,3,4, and 6. The total usable data is reduced to 100.68 ks after removing periods of potential flares and elevated background. Figure 1 shows the resulting *Chandra* X-ray (0.5–6.0 keV) image. The X-ray image has been smoothed with a Gaussian kernel with radius $r_k = 2.5''$.

3 Diffuse emission and the search for a dark matter signature

Based on the high mass-to-light ratio (~ 700) inferred by **(author?)** [33], Willman 1 has emerged as an attractive target for indirect DM searches [27]. Yet, to date no DM signal has been observed in sensitive observations of Willman 1 at energies > 100 MeV [7, 8].

[1] http://cxc.harvard.edu/ciao/threads/acisclean vf/

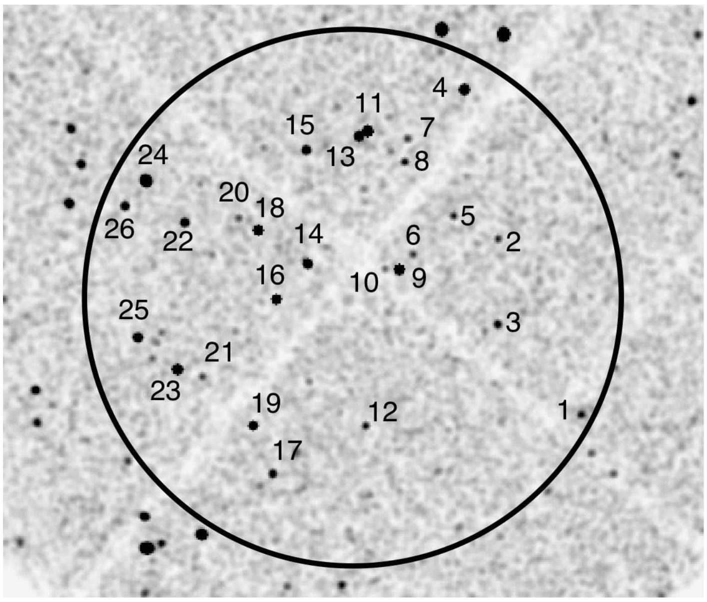

Figure 1. *Chandra* ACIS-I image of Willman 1 in the 0.5–6.0 keV energy range. The X-ray image has been smoothed with a Gaussian kernel with radius $r_k = 2.5''$. Identified sources are marked following the labels adopted in Table 1. The circle is centred on RA. $10^{\rm h}49^{\rm m}22\overset{\rm s}{.}3$, Dec. $+51°03'03''$ and drawn with a $5'$ radius. The half-light radius corresponds to $r_{1/2} = 1.9'$. Notice that the placement falls near the intersection of the chip gaps.

In X-rays, one expect that the diffuse emission in Willman 1 will be dominated either by an unresolved point source population or by a complex gaseous component [34]. However, there is also a possibility that the DM halo of Willman 1 might produce a detectable X-ray flux via sterile neutrino decay. The principal decay channel for sterile neutrinos is into three light active neutrinos. Nonetheless, there is a potentially detectable radiative decay channel in the X-ray band, whereby a lighter active neutrino and a X-ray photon are produced with a slow mean decay on the order of the lifetime of the Universe. The former is a two-body decay, meaning that the resulting photon energy distribution is characterised by a spectral line with a broadening due to the velocity dispersion of the original sterile neutrino population.

In order to survey the diffuse emission, we excised all point sources within the inner $5'$ of Willman 1. Due to an unfortunate placement of the object within the ACIS footprint, the diffuse emission is missing a critical section of the inner core of Willman 1 and extends over four distinct ACIS-I CCDs with distinct gains (see Figure 1). In order to avoid significant intrachip variations, we excluded 32 pixels to each side of the CCD edges. Visual examination of the resulting X-ray image does not reveal prominent diffuse emission that would give away a rich globular cluster core. Given the intrachip gain fluctuations across the CCDs, it is not straightforward to ascertain the significance of the counts within the inner $5'$ of Willman 1. We note however that the limited signal-to-noise ratio and placement across four CCDs cannot ensure that the detected counts correspond to diffuse emission specific to Willman 1. Rather the counts might result from Poisson fluctuations in the background count rate.

On the other hand, it is possible to derive upper limits on the diffuse emission after subtracting the background contribution at this position. The spectrum of the diffuse emission was rendered from a $5'$ radius circle at the nominal position of Willman 1 of RA. $10^{\rm h}49^{\rm m}22\overset{\rm s}{.}3$,

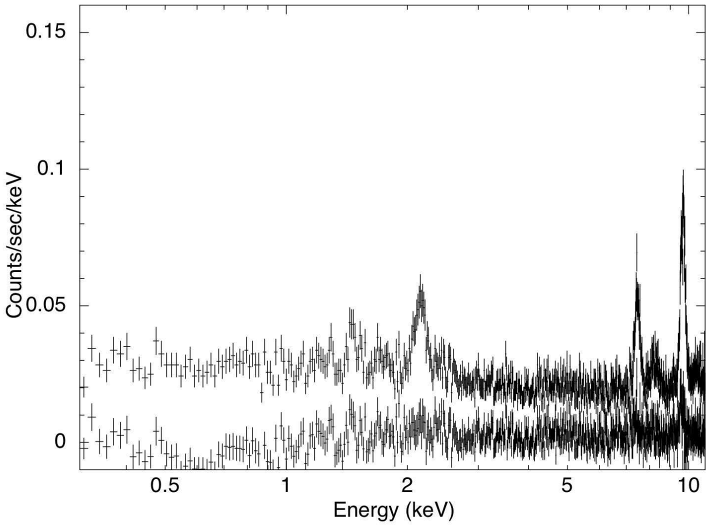

Figure 2. *Chandra* ACIS-I spectrum extracted from a $5'$ radius circle centred on Willman 1 as described in the text. *Top:* Data prior to removal of the background. Instrumental line features include Si K α (1.74 keV), Au M α, β (2.1–2.2 keV), Ni K α (7.47 keV), and Au L α (9.67 keV). *Bottom:* Spectrum after background subtraction.

Dec. $+51°03'03''$ and corrected with the standard reprojected blank-sky background.[2] The final step consisted in a renormalization of the background spectrum to match the 9.0–12.0 keV count rate of the Willman 1 exposure. Figure 2 shows the spectrum before and after subtraction of the background. Prior to subtraction, the spectrum is dominated by prominent instrumental line features that originate from fluorescence of material in the telescope including Si K α (1.74 keV), Au M α, β (2.1–2.2 keV), Ni K α (7.47 keV), and Au L α (9.67 keV). The instrumental features are largely removed after subtracting the background.

In order to establish upper limits to the emission of DM in the energy range covered by the observation, we fit the spectrum in steps of 0.1 keV with the appropriate Gaussian width σ required to match the spectral resolution at each step. This emulates the procedure outlined in previous analyses of *Chandra* data [35, 36]. We next proceeded to derive limits coming from a DM halo composed of sterile neutrino particles with rest mass 1.6 keV $< m_\nu <$ 16.0 keV as a function of mixing angle θ adopting the formalism of **(author?)** [30],

$$F_{line} = 5.15 \sin^2\theta \left(\frac{m_s}{keV}\right)^4 f_s M_7 d_{100}^{-2} cm^{-2} s^{-1} \tag{3.1}$$

where sterile neutrinos with mass m_s produce photons at a given line energy $E_{line} = m_s/2$, M_7 is the projected DM mass of Willman 1 in units of $10^7 M_\odot$, f_s is the fraction of DM in sterile neutrino form and d_{100} is the distance to Willman 1 in units of 100 kpc. For the actual calculations, we assume that the DM is composed by sterile neutrinos only ($f_s = 1$), a heliocentric distance $d_{100} = 0.38$ [32] and a projected DM mass $M_7 = 0.2$ [30]. Figure 4 shows the resulting sterile neutrino parameter space ruled out by the *Chandra* observation.

[2] http://cxc.harvard.edu/ciao/threads/acisbackground/index.sl.html

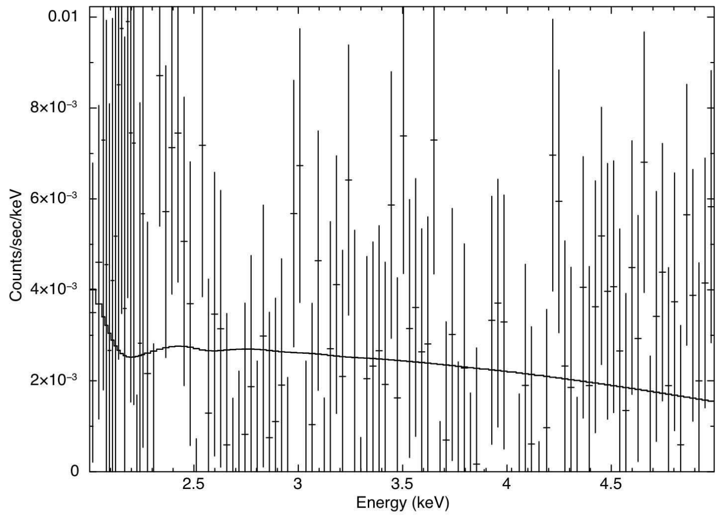

Figure 3. *Chandra* ACIS spectrum of the diffuse component of Willman 1 in the 2.0-5.0 keV energy range and best-fitting absorbed power-law model as described in the text.

Except for some minor differences, our results for the parameter space are consistent with the results originally reported by **(author?)** [30].

However, we differ from **(author?)** [30] in that we find no evidence for a purported line detection at 2.51 keV with a line flux $f_{line} = 3.53 \times 10^{-6}$ photons cm^{-2} s^{-1}. Figure 3 shows the background-subtracted ACIS spectrum in the 2.0–5.0 keV energy region. An absorbed power-law model fixed at the Galactic H I column density $N_{\rm H} = 1.2 \times 10^{20}$ cm^{-2} and photon index $\Gamma = 1.0 \pm 0.6$ appears to accommodate the data ($\chi^2_\nu = 0.86$). There is an excess around 2.3–2.5 keV, but the inclusion of a Gaussian line with the properties reported in **(author?)** [30] does not improve the fit ($\chi^2_\nu = 0.85$). Leaving the power-law index to be a free parameter and allowing the Gaussian line centroid wander in the 2.0–3.0 keV energy yields an unrealistic $\Gamma = -1.2 \pm 0.7$ with a Gaussian line centred at 2.2 keV. The latter is most likely due to the instrumental Au M α, β (2.1–2.2 keV) line and highlights the difficulties with reported line detections in and around this region. Thus, while we cannot rule out weak emission between 2.3 and 2.5 keV, we find that a power-law model provides a satisfactory fit without the need for the Gaussian line reported by **(author?)** [30].

Upon closer inspection of Figure 1 in **(author?)** [30] we notice spectral residuals in the vicinity of the aforementioned instrumental lines of Au M α, β (2.1–2.2 keV), Ni K α (7.47 keV), and Au L α (9.67 keV). We face similar issues in our analysis that seem entirely consistent with a diffuse emission signal heavily dominated by background spectrum [see also 28]. In such circumstances, it is possible that a deficient subtraction of the Au M α, β (2.1–2.2 keV) instrumental line or calibration issues at $E < 2.3$ keV will start to carve the silhouette of a spectral line around 2.4–2.5 keV that might result in the finding reported in **(author?)** [30]. In addition, it is difficult to discard that intrachip gain variations may conspire to mimic an emission line. It is important to recall that spurious X-ray line detections have a curious history in the literature [37, 38]. Henceforth, one must be careful when dealing with marginal

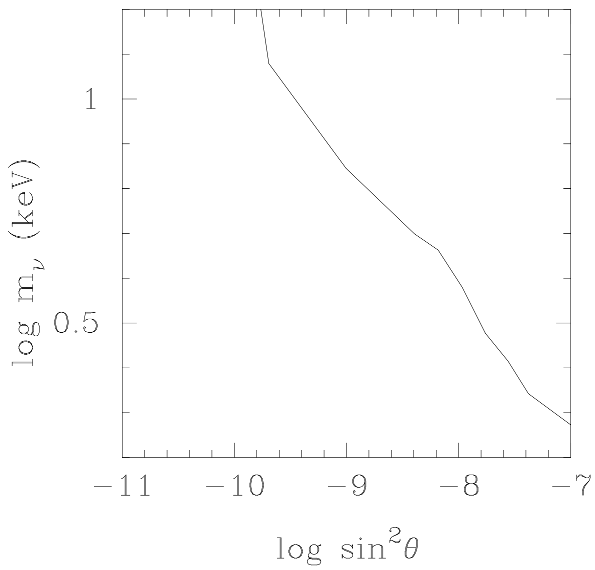

Figure 4. Parameter space constraints for the sterile neutrino. The region to the right of the contour is ruled out by the *Chandra* observation of Willman 1.

detections [39].

Even if one wants to advocate the reality of a line at 2.51 keV, a direct DM connection suffers from a fatal flaw in that it falls at a location matching the rest-frame of helium-like sulphur ion S XV α located at 2.45 keV [40]. This astrophysical line is routinely detected in plasmas with temperatures $\sim 10^{6-7}$ K [41, 42]. Consequently, it seems more plausible that one is detecting sulphur emission from a hot supernova remnant or a highly-ionised wind region either at Willman 1 itself or at an intervening location to the object, rather than the exotic signature of DM.

4 X-ray point source population

Apart from allowing access to the extended emission, the *Chandra* resolution is sufficiently detailed to study the X-ray point source population in the field of Willman 1. For the purposes of this work, we searched for point sources within the central $5'$ of Willman 1 using the CIAO tool *celldetect*. This corresponds to a physical size of 55 pc assuming a distance of 38 kpc. This region encompasses the half-light radius of Willman 1 estimated to be $r_{1/2} = 1.9'$ [32]. Figure 1 shows all 26 detections with more than 15 net counts in the 0.5–6.0 keV energy range, which translates into a luminosity limit for point-like sources of 2.7×10^{32} erg s^{-1}. Ten of the sources are on the I1 chip, seven on the I2 chip, six on the I0 chip, and three on the I3 chip.

X-ray counts were extracted within a $2.5''$ radius circles centred on the source location. The counts were then separated in three different energy ranges: a *soft* band (0.5–1.5 keV), a *medium* band (0.5-4.5 keV), and a *hard* band (1.5-6.0 keV). Finally, we estimated net counts using source-free background regions in the corresponding individual chip. The source labels, positions, and net counts in three separate energy bands are listed in Table 1. A complementary search for optical counterparts was performed cross-checking source positions with *SDSS DR7* catalogue [43]. The association required the angular distance between *Chandra*

Source Label	Name	R.A. (J2000.0)	Dec. (J2000.0)	Net Counts 0.5 – 1.5 keV	0.5 – 4.5 keV	1.5 – 6.0 keV
1	CXOU J104855.4+510053	10 48 55.4	+51 00 53.0	1±1	14±4	20±5
2	CXOU J104905.1+510409	10 49 05.1	+51 04 09.6	1±1	16±4	20±5
3	CXOU J104905.2+510234	10 49 05.2	+51 02 34.5	15±4	29±5	17±4
4	CXOU J104909.1+510657	10 49 09.1	+51 06 57.1	94±10	171±13	83±9
5	CXOU J104910.3+510435	10 49 10.3	+51 04 35.8	15±4	20±5	5±2
6	CXOU J104915.1+510353	10 49 15.1	+51 03 53.2	6±3	14±4	9±3
7	CXOU J104915.9+510602	10 49 15.9	+51 06 02.2	9±3	17±4	8±3
8	CXOU J104916.2+510536	10 49 16.2	+51 05 36.6	18±4	26±5	10±3
9	CXOU J104916.8+510335	10 49 16.8	+51 03 35.6	89±9	161±13	83±9
10	CXOU J104918.5+510337	10 49 18.5	+51 03 37.0	7±3	12±4	8±3
11	CXOU J104920.6+510610	10 49 20.6	+51 06 10.6	183±14	291±17	124±11
12	CXOU J104920.8+510041	10 49 20.8	+51 00 41.3	15±4	22±5	10±3
13	CXOU J104921.6+510605	10 49 21.6	+51 06 05.1	46±7	81±9	39±6
14	CXOU J104927.7+510341	10 49 27.7	+51 03 41.5	27±5	66±8	39±6
15	CXOU J104927.8+510549	10 49 27.8	+51 05 49.3	28±5	55±7	33±6
16	CXOU J104931.4+510302	10 49 31.4	+51 03 02.5	58±8	100±10	47±7
17	CXOU J104931.8+505947	10 49 31.8	+50 59 47.0	12±4	33±6	24±5
18	CXOU J104933.6+510420	10 49 33.6	+51 04 20.0	48±7	112±11	70±8
19	CXOU J104934.1+510041	10 49 34.1	+51 00 41.1	28±5	61±8	39±6
20	CXOU J104935.9+510433	10 49 35.9	+51 04 33.2	4±2	13±4	11±3
21	CXOU J104940.2+510136	10 49 40.2	+51 01 36.0	4±2	13±4	14±4
22	CXOU J104942.3+510428	10 49 42.3	+51 04 28.1	36±6	57±8	24±5
23	CXOU J104943.1+510144	10 49 43.1	+51 01 44.1	34±6	178±13	157±13
24	CXOU J104946.9+510514	10 49 46.9	+51 05 14.7	154±12	316±18	193±14
25	CXOU J104947.8+510219	10 49 47.8	+51 02 19.7	31±6	78±9	57±8
26	CXOU J104949.4+510446	10 49 49.4	+51 04 46.8	26±5	43±7	19±4

Table 1. X-ray sources identified within the central $5'$ of Willman 1. X-ray counts were extracted within a $2.5''$ radius circles centred on the source location.

Source Label	Name	Optical match	Offset ($''$)	Classification †	Redshift ‡
4	CXOU J104909.1+510657	SDSS J104909.10+510657.0	0.1	Star	-
8	CXOU J104916.2+510536	SDSS J104916.19+510536.6	0.1	Galaxy	-
11	CXOU J104920.6+510610	SDSS J104920.62+510610.5	0.2	Star	-
12	CXOU J104920.8+510041	SDSS J104920.85+510041.3	0.5	QSO ∗	2.8
13	CXOU J104921.6+510605	SDSS J104921.64+510605.1	0.4	QSO ∗	1.6
16	CXOU J104931.4+510302	SDSS J104931.40+510302.6	0.2	QSO ∗	2.1
17	CXOU J104931.8+505947	SDSS J104931.79+505946.9	0.1	Galaxy	-
24	CXOU J104946.9+510514	SDSS J104946.90+510514.3	0.4	QSO ∗	0.8
25	CXOU J104947.8+510219	SDSS J104947.85+510220.0	0.6	Galaxy	-
26	CXOU J104949.4+510446	SDSS J104949.36+510446.6	0.3	Star	-

Table 2. X-ray sources with optical matches within the central $5'$ of Willman 1. † According to **(author?)** [43]. ‡ Photometric redshift from **(author?)** [44]. ∗ Photometric classification from **(author?)** [44]

and *SDSS* catalogue sources to be less than $2.5''$. This criterion produces 10 optical matches out of the total sample of 26 sources. According to *SDSS* object classification, 3 are categorized as stars and 3 as galaxies. The remainder 4 matches are listed as part of the *NBCK* catalogue of photometrically selected quasar candidates [44]. Sources with optical matches are summarised in Table 2. It is important to emphasise that *SDSS* optical sources have been tentatively labelled based on colours and that no reliable spectroscopic classifications were available at the time of this writing.

The principal obstacle in sorting out whether any individual point source in the field

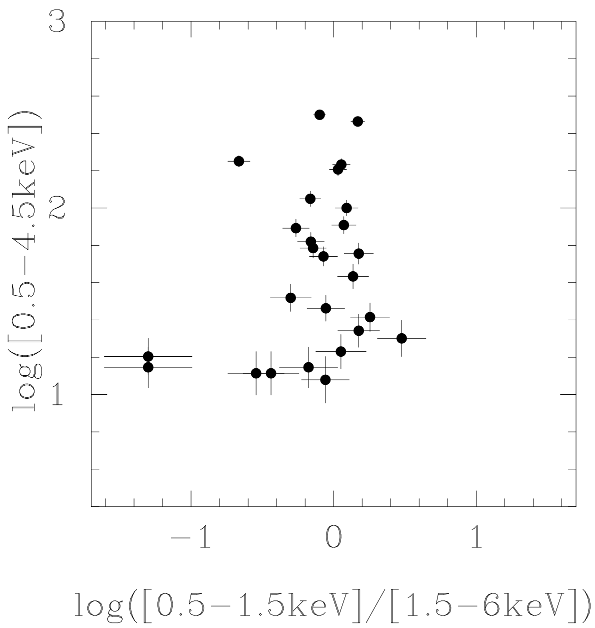

Figure 5. X-ray colour-magnitude diagram for 26 sources detected within the inner 5′ of Willman 1.

represents a *bona fide* member of Willman 1 is the inescapable presence of background active galactic nuclei (AGN) and galaxies in the field [45, 46]. It turns out to be extremely difficult to distinguish the source identity whenever the number of predicted background AGN matches the observed number of sources in the field [47]. In this instance, a detection limit of 15 net counts in the 0.5–6 keV energy range corresponds to a limiting flux 6×10^{-16} erg cm^{-2} s^{-1} in the 0.5–2.0 keV band, adopting an X-ray power spectral index $\Gamma = 1.4$ and a Galactic H I column density $N_{\rm H} = 1.2 \times 10^{20}$ cm^{-2}. Using the latest AGN counts from the *Chandra* Deep Field-South (CDFS) reported by **(author?)** [46], we expect an average of 24 ± 3 background AGN for a field of this size to our limiting flux in the 0.5–2.0 keV band. Our detection of 26 sources does not exceed significantly the CDFS prediction. As a result, the majority of sources found are most likely background AGN.

Since this result relies on the adopted background source count, we proceeded to evaluate the variability and colour of the sample. The presence of binary systems might be exposed through the detection of strong variability [48]. According to the CIAO tool *glvary*, there are no definite variables among the point sources. Similarly, the location of a source in an X-ray colour magnitude diagram (CMD) might be a powerful way to infer the presence of binary systems in a field [49]. In particular, certain CVs/LMXBs will depart from AGN and become outliers in the colour distribution. In Figure 5 we plot the logarithm of the 0.5–4.5 keV counts versus the logarithm of the ratio of 0.5–1.5 keV and 1.5–6.0 keV net counts. Note that the majority of the sources tend to gather around the center of the diagram where it is difficult to tell binary systems and AGN apart. However, the void in the upper right corner of the diagram probably rules out the presence of LMXBs in quiescence [48]. The two hard sources to the left of the diagram could indicate heavily obscured AGN but the reduced number of counts prevents a formal identification. Therefore, the colour analysis fails to discover any apparent binary system in the field as expected by our estimation.

Additional clues about the nature of the point like population might be gained from the examination of the actual spectra of the sources. For this reason, spectra were generated for all the sources with 50 or more detected counts in the 0.5–6.0 keV energy band. This criterion leaves 13 out of the total sample of 26 sources. The counts for each source were grouped using the CIAO tool *dmgroup* such that there are 10 counts per bin. By default, we adopted a power-law model spectral fit within XSPEC [50] with the absorption fixed at the Galactic value $N_{\rm H} = 1.2 \times 10^{20}$ cm^{-2}. Power law fits with indices $1.2 < \Gamma < 2$ are acceptable ($\chi^2_\nu < 1.5$) to all sources, except source 14. For the latter a blackbody or models with substantial internal absorption provide better fits. However, it is difficult to make a final spectral classification for that source. Overall, the spectral results are consistent with the properties of background AGN in such a field. We note that there is also a non-negligible probability that a handful of coronal emitting stars in the foreground could be superposed by chance along the line of sight [51].

Last but not least, the number of expected X-ray binary systems in Willman 1 can be estimated theoretically. We computed the so-called encounter rate following **(author?)** [52] and considering a core radius $r_c = 1.5'$ and density $\rho_0 \sim 1 \times 10^{-2} L_\odot/pc^{-3}$ [33]. Applying the normalisation in **(author?)** [53] we derive a very low probability estimate ($p \sim \mathcal{O}(10^{-7})$) of finding X-ray binary systems at a luminosity over $4 \times 10^{30} erg\ s^{-1}$. Given that our luminosity limit falls two orders of magnitude above, the probability estimate must be considered as an upper limit and therefore one would not expect to detect any X-ray binary system belonging to Willman 1 in this observation. Nevertheless the assumptions made in order to infer the binary rate are based on the daring hypothesis that Willman 1 density has remained constant throughout its evolution. Willman 1's unusual kinematics challenges any current model of tidally disrupted or ordered rotating system and point towards a significant tidal evolution which could have stripped a noteworthy fraction of its stellar component [54]. The initial stellar density of the system could have been such that binary systems were formed more efficiently in the past. Consequently the probability estimate should be taken *cum grano salis* since Willman 1 past evolution may have played a crucial role in binary formation. But since it might be nearly impossible to derive the past encounter rate from current dynamical structure, there is no reason to conclude that any significant fraction of the point source population in the field is associated with Willman 1.

5 Summary and conclusions

Adopting an estimated distance of 38 kpc, it might be the case that the bulk of sources connected with Willman 1 lies below our luminosity limit of 10^{32} erg s^{-1} in the 0.5–2.0 keV energy band, as in the case of globular cluster GLIMPSE-C01 [55]. However, our encounter rate calculations indicate a very low probability of finding candidate binaries within Willman 1. Combined with existing optical imaging, the *Chandra* observation of Willman 1 could help purge possible member stars of any AGN contaminants/stellar interlopers. Furthermore, further analysis might help us investigate how will the X-ray point source population influence the prospects of detecting a dark matter signal from Willman 1 with gamma-ray measurements.

Given the existing sterile neutrino limits, it might be wise to concentrate on the detectability of the sterile neutrino with future X-ray experiments [56] as it will be difficult to improve current measurements with the existing instrumentation [57]. In particular, making the case for future calorimeter experiments that could definitely detect it or exclude it as a DM candidate (F. Paerels, private communication). We have shown here that any viable indirect search for DM in this energy range must deal not only with possible overlap with instrumental lines in the spectrum [36], but also with possible contamination from intervening plasma lines that may mask a DM origin. We caution that extraordinary claims related to DM should be backed by outstanding observational evidence [58].

With the Large Hadron Collider (LHC) and other laboratory experiments coming online, it might be possible to achieve a direct detection of the particles responsible for DM. However, any direct detection in the laboratory will then have to be followed by confirmation or dismissal of sameness in an astrophysical context. Based on the present study, Willman 1 continues to hold a select place among targets to conduct such searches. It is worth noting that within the inner $5'$ radius circle of Willman 1, there are no radio sources at 1.4 GHz in the NRAO VLA Sky Survey (NVSS) source catalog [59]. Moreover, we have shown that the point source population to a limiting 0.5–2.0 keV X-ray flux of 6×10^{-16} erg cm^{-2} s^{-1} is consistent with background AGN and/or foreground stars. Pending a final verdict regarding the kinematic distribution of Willman 1 [54], the available data from radio through X-rays thus make Willman 1 a notable candidate for the eventual astrophysical verification of a DM particle.

Acknowledgments

We are indebted to an anonymous colleague for careful reading of the original version. We thank all the members of Grupo de Altas Energías (GAE) at the Universidad Complutense de Madrid for stimulating discussions. N.M. acknowledges support from the Spanish Ministry of Science and Innovation through a Ramón y Cajal fellowship. We also acknowledge support from the Consolider-Ingenio 2010 Programme under grant MULTIDARK CSD2009-00064.

References

[1] **WMAP** Collaboration, E. Komatsu *et. al.*, *Seven-Year Wilkinson Microwave Anisotropy Probe (WMAP) Observations: Cosmological Interpretation*, *Astrophys.J.Suppl.* **192** (2011) 18, [astro-ph.CO/1001.4538].

[2] R. Gaitskell, *Direct detection of dark matter*, *Ann.Rev.Nucl.Part.Sci.* **54** (2004) 315–359.

[3] G. Bertone, D. Hooper, and J. Silk, *Particle dark matter: Evidence, candidates and constraints*, *Phys.Rept.* **405** (2005) 279–390, [hep-ph/0404175].

[4] G. Kane and S. Watson, *Dark Matter and LHC: What is the Connection?*, *Mod.Phys.Lett.* **A23** (2008) 2103–2123, [hep-ph/0807.2244].

[5] D. G. Cerdeño and A. M. Green, *Direct detection of WIMPs*, pp. 347–+. Cambridge University Press, 2010.

[6] G. Bertone and D. Merritt, *Dark matter dynamics and indirect detection*, *Mod.Phys.Lett.* **A20** (2005) 1021, [astro-ph/0504422].

[7] **MAGIC** Collaboration, E. Aliu *et. al.*, *MAGIC upper limits on the VHE gamma-ray emission from the satellite galaxy Willman 1*, *Astrophys. J.* **697** (2009) 1299–1304, [astro-ph/0810.3561].

[8] A. Abdo, M. Ackermann, M. Ajello, W. Atwood, L. Baldini, *et. al.*, *Observations of Milky Way Dwarf Spheroidal galaxies with the Fermi-LAT detector and constraints on Dark Matter models*, *Astrophys.J.* **712** (2010) 147–158, [astro-ph.CO/1001.4531].

[9] B. Anderson, M. Kuhlen, J. Diemand, R. P. Johnson, and P. Madau, *Fermi-LAT Sensitivity to Dark Matter Annihilation in Via Lactea II Substructure*, *Astrophys.J.* **718** (2010) 899–904, [astro-ph.HE/1006.1628].

[10] J. Chang, J. Adams, H. Ahn, G. Bashindzhagyan, M. Christl, *et. al.*, *An excess of cosmic ray electrons at energies of 300-800 GeV*, *Nature* **456** (2008) 362–365.

[11] **PAMELA** Collaboration, O. Adriani *et. al.*, *An anomalous positron abundance in cosmic rays with energies 1.5-100 GeV*, *Nature* **458** (2009) 607–609, [astro-ph/0810.4995].

[12] **Fermi-LAT** Collaboration, A. A. Abdo *et. al.*, *Measurement of the Cosmic Ray e+ plus e- spectrum from 20 GeV to 1 TeV with the Fermi Large Area Telescope*, *Phys.Rev.Lett.* **102** (2009) 181101, [astro-ph.HE/0905.0025].

[13] **HESS** Collaboration, F. Aharonian *et. al.*, *Probing the ATIC peak in the cosmic-ray electron spectrum with H.E.S.S*, *Astron.Astrophys.* **508** (2009) 561, [astro-ph.HE/0905.0105].

[14] H. E. Haber and G. L. Kane, *The Search for Supersymmetry: Probing Physics Beyond the Standard Model*, *Phys.Rept.* **117** (1985) 75–263.

[15] L. Bergström, T. Bringmann, M. Eriksson, and M. Gustafsson, *Gamma rays from kaluza-klein dark matter*, *Phys. Rev. Lett.* **94** (Apr, 2005) 131301.

[16] J. L. Feng, *Dark Matter Candidates from Particle Physics and Methods of Detection*, *Ann.Rev.Astron.Astrophys.* **48** (2010) 495, [astro-ph.CO/1003.0904].

[17] S. Dodelson and L. M. Widrow, *Sterile-neutrinos as dark matter*, *Phys.Rev.Lett.* **72** (1994) 17–20, [hep-ph/9303287].

[18] T. Asaka and M. Shaposhnikov, *The nuMSM, dark matter and baryon asymmetry of the universe*, *Phys.Lett.* **B620** (2005) 17–26, [hep-ph/0505013].

[19] R. K. de Naray, G. D. Martinez, J. S. Bullock, and M. Kaplinghat, *The Case Against Warm or Self-Interacting Dark Matter as Explanations for Cores in Low Surface Brightness Galaxies*, *Astrophys.J.* **710** (2009) 161, [astro-ph.CO/0912.3518].

[20] K. Abazajian, G. M. Fuller, and W. H. Tucker, *Direct detection of warm dark matter in the X-ray*, *Astrophys.J.* **562** (2001) 593–604, [astro-ph/0106002].

[21] A. Dolgov and S. Hansen, *Massive sterile neutrinos as warm dark matter*, *Astropart.Phys.* **16** (2002) 339–344, [hep-ph/0009083].

[22] H. Yuksel, J. F. Beacom, and C. R. Watson, *Strong Upper Limits on Sterile Neutrino Warm Dark Matter*, *Phys.Rev.Lett.* **101** (2008) 121301, [astro-ph/0706.4084].

[23] G. B. Gelmini, E. Osoba, and S. Palomares-Ruiz, *Inert-Sterile Neutrino: Cold or Warm Dark Matter Candidate*, *Phys.Rev.* **D81** (2010) 063529, [hep-ph/0912.2478].

[24] B. Willman, M. R. Blanton, A. A. West, J. J. Dalcanton, D. W. Hogg, *et. al.*, *A New Milky Way companion: Unusual globular cluster or extreme dwarf satellite?*, *Astron.J.* **129** (2005) 2692–2700, [astro-ph/0410416].

[25] **SDSS** Collaboration, V. Belokurov *et. al.*, *Cats and Dogs, Hair and A Hero: A Quintet of New Milky Way Companions*, *Astrophys.J.* **654** (2007) 897–906, [astro-ph/0608448].

[26] J. D. Simon, M. Geha, Q. E. Minor, G. D. Martinez, E. N. Kirby, *et. al.*, *A Complete Spectroscopic Survey of the Milky Way Satellite Segue 1: The Darkest Galaxy*, *Astrophys.J. (submitted)* (2010) [astro-ph.GA/1007.4198].

[27] L. E. Strigari, S. M. Koushiappas, J. S. Bullock, M. Kaplinghat, J. D. Simon, M. Geha, and B. Willman, *The Most Dark-Matter-dominated Galaxies: Predicted Gamma-Ray Signals from the Faintest Milky Way Dwarfs*, *Astrophys.J.* **678** (2008) 614.

[28] A. Boyarsky, O. Ruchayskiy, D. Iakubovskyi, M. G. Walker, S. Riemer-Sorensen, *et. al.*, *Searching for dark matter in X-rays: how to check the dark matter origin of a spectral feature*, *Mon.Not.Roy.Astron.Soc.* **407** (2010) 1188–1202, [astro-ph.CO/1001.0644].

[29] M. Loewenstein, A. Kusenko, and P. L. Biermann, *New Limits on Sterile Neutrinos from*

Suzaku Observations of the Ursa Minor Dwarf Spheroidal Galaxy, *Astrophys.J.* **700** (2009) 426–435, [astro-ph/0812.2710].

[30] M. Loewenstein and A. Kusenko, *Dark Matter Search Using Chandra Observations of Willman 1, and a Spectral Feature Consistent with a Decay Line of a 5 keV Sterile Neutrino*, *Astrophys.J.* **714** (2010) 652–662, [astro-ph.H/0912.0552].

[31] N. Mirabal, *Swift observation of Segue 1: constraints on sterile neutrino parameters in the darkest galaxy*, *Mon.Not.Roy.Astron.Soc.* **409** (Nov., 2010) L128–L131, [astro-ph.HE/1010.4706].

[32] B. Willman, M. Masjedi, D. W. Hogg, J. J. Dalcanton, D. Martinez-Delgado, M. Blanton, A. A. West, A. Dotter, and B. Chaboyer, *Willman 1 - A Galactic Satellite at 40 kpc With Multiple Stellar Tails*, *ArXiv Astrophysics e-prints* (Mar., 2006) [astro-ph/].

[33] N. Martin, R. Ibata, S. Chapman, M. Irwin, and G. Lewis, *A Keck/DEIMOS spectroscopic survey of faint Galactic satellites: Searching for the least massive dwarf galaxies*, *Mon.Not.Roy.Astron.Soc.* **380** (2007) 281–300, [astro-ph/0705.4622].

[34] C. Hui, K. Cheng, and R. E. Taam, *Diffuse X-ray emission in globular cluster cores*, *Astrophys.J.* **700** (2009) 1233–1241, [astro-ph.HE/0905.2908].

[35] N. Mirabal, F. Paerels, and J. Halpern, *High resolution grating spectroscopy of GRB 020405 with Chandra LETGS*, *Astrophys.J.* **587** (2003) 128–134, [astro-ph/0209516].

[36] S. Riemer-Sorensen, S. H. Hansen, and K. Pedersen, *Sterile neutrinos in the Milky Way: Observational constraints*, *Astrophys.J.* **644** (2006) L33–L36, [astro-ph/0603661].

[37] M. Sako, F. A. Harrison, and R. Rutledge, *A Search for discrete x-ray spectral features in a sample of bright gamma-ray burst afterglows*, *Astrophys.J.* **623** (2005) 973–999, [astro-ph/0406210].

[38] S. Vaughan and P. Uttley, *On the evidence for narrow, relativistically shifted X-ray lines*, *Mon.Not.Roy.Astron.Soc.* **390** (Oct., 2008) 421–428, [astro-ph/0807.4806].

[39] R. Protassov, D. A. van Dyk, A. Connors, V. L. Kashyap, and A. Siemiginowska, *Statistics, Handle with Care: Detecting Multiple Model Components with the Likelihood Ratio Test*, *Astrophys.J.* **571** (May, 2002) 545–559, [astro-ph/0201547].

[40] J. C. Raymond and B. W. Smith, *Soft X-ray spectrum of a hot plasma*, *Astrophys.J.Suppl.* **35** (1977) 419–439.

[41] U. Hwang *et. al.*, *A Million Second Chandra View of Cassiopeia A*, *Astrophys.J.Lett.* **615** (Nov., 2004) L117–L120, [astro-ph/0409760].

[42] D. Henley, M. Corcoran, J. Pittard, I. Stevens, K. Hamaguchi, *et. al.*, *Chandra X-ray Grating Spectrometry of Eta Carinae near X-ray Minimum: I. Variability of the Sulfur and Silicon Emission Lines*, *Astrophys.J.* **680** (2008) 705, [astro-ph/0801.4779].

[43] **SDSS** Collaboration, K. N. Abazajian *et. al.*, *The Seventh Data Release of the Sloan Digital Sky Survey*, *Astrophys.J.Suppl.* **182** (2009) 543–558, [astro-ph/0812.0649].

[44] G. T. Richards, A. D. Myers, A. G. Gray, R. N. Riegel, R. C. Nichol, *et. al.*, *Efficient Photometric Selection of Quasars from the Sloan Digital Sky Survey: II. 1,000,000 Quasars from Data Release Six*, *Astrophys.J.Suppl.* **180** (2009) 67–83, [astro-ph/0809.3952].

[45] R. Giacconi, P. Rosati, P. Tozzi, M. Nonino, G. Hasinger, *et. al.*, *First results from the x-ray and optical survey of the Chandra Deep Field South*, *Astrophys.J.* **551** (2001) 624–634, [astro-ph/0007240].

[46] B. Luo, F. Bauer, W. Brandt, D. Alexander, B. Lehmer, *et. al.*, *The Chandra Deep Field-South Survey: 2 Ms Source Catalogs*, *Astrophys.J.Suppl.* **179** (2008) 19–36, [astro-ph/0806.3968].

[47] G. Ramsay and K. Wu, *A search for stellar X-ray sourcesin the Sagittarius and Carina dwarf*

galaxies. 1. X-ray observations, *Astron.Astrophys.* **459** (2006) 777–781, [astro-ph/0609116].

[48] C. Heinke, J. Grindlay, P. Edmonds, D. Lloyd, S. Murray, *et. al.*, *A chandra x-ray study of the globular cluster m80*, *Astrophys.J.* **598** (2003) 516–526, [astro-ph/0305443].

[49] J. E. Grindlay, C. Heinke, P. D. Edmonds, and S. S. Murray, *High-Resolution X-ray Imaging of a Globular Cluster Core: Compact Binaries in 47Tuc*, *Science* **292** (June, 2001) 2290–2295, [astro-ph/0105528].

[50] K. A. Arnaud, *Astronomical Data Analysis Software and Systems V*, vol. 101 of *Conference Series*. Astron. Soc. Pac., San Francisco, 1996.

[51] D. Haggard, A. M. Cool, and M. B. Davies, *A Chandra Study of the Galactic Globular Cluster Omega Centauri*, *Astrophys.J.* **697** (2009) 224–236, [astro-ph.HE/0902.2397].

[52] F. Verbunt, *Binary Evolution and Neutron Stars in Globular Clusters*, vol. 296 of *Conference Series*. Astron. Soc. Pac., San Francisco, 2003.

[53] D. Pooley, W. Lewin, S. Anderson, H. Baumgardt, A. Filippenko, *et. al.*, *Dynamical formation of close binary systems in globular clusters*, *Astrophys.J.* **591** (2003) L131–L134, [astro-ph/0305003].

[54] B. Willman, M. Geha, J. Strader, L. E. Strigari, J. D. Simon, *et. al.*, *Willman 1 - a probable dwarf galaxy with an irregular kinematic distribution*, *Astron.J. (submitted)* (2010) [astro-ph.GA/1007.3499].

[55] D. Pooley, S. Rappaport, A. Levine, E. Pfahl, and J. Schwab, *Chandra X-Ray Observation of the Globular Cluster GLIMPSE-C01*, *Astrophys.J. (submitted)* (2007) [astro-ph/0708.3365].

[56] J. den Herder, A. Boyarsky, O. Ruchayskiy, K. Abazajian, C. Frenk, *et. al.*, *The Search for decaying Dark Matter*, astro-ph.C/0906.1788.

[57] K. Abazajian, *Detection of Dark Matter Decay in the X-ray*, in *astro2010: The Astronomy and Astrophysics Decadal Survey*, vol. 2010 of *ArXiv Astrophysics e-prints*, pp. 1–+, 2009. astro-ph.CO/0903.2040.

[58] C. Sagan, *Cosmos*. Random House, New York, 1980.

[59] J. J. Condon, W. Cotton, E. Greisen, Q. Yin, R. Perley, *et. al.*, *The NRAO VLA Sky survey*, *Astron.J.* **115** (1998) 1693–1716.